Technical Note

Experiments Using a Novel Penetrometer to Assess Changing Strength of Clay during Remolding and Reconsolidation

Fauzan Sahdi[1]; David J. White[2]; and Christophe Gaudin[3]

Abstract: The process of remolding and subsequent recovery of soil shear strength is a common geotechnical problem, especially in the offshore environment, where foundations and pipelines are subjected to intermittent operational and environmental loads. A novel vertically oriented penetrometer (VOP) was used in a centrifuge testing program to study the changing strength of normally consolidated kaolin from successive disturbance and reconsolidation events. The VOP is used to determine soil shear strength via an interpretation akin to the laterally loaded pile. The test series involved cyclic movement of the VOP at velocities ranging from 0.3 to 30 mm/s, with a corresponding 100-fold variation in the duration of each cycle. For the VOP tests at low velocities with high cyclic periods, the soil resistance initially reduces, but then shows an increase that scales with the elapsed time, indicating reconsolidation. Ultimately, if the cycling continues for sufficient time, the recovery in strength from reconsolidation can exceed the weakening from remolding. A previously published framework using critical-state soil mechanics concepts is shown to capture the changing resistance well. **DOI: 10.1061/(ASCE)GT.1943-5606.0001637.** © *2016 American Society of Civil Engineers.*

Introduction

Many geotechnical problems involve episodes of gross undrained soil disturbance. In contractile fine-grained soils, this disturbance causes a decrease in effective stress due to the accumulation of positive excess pore pressure. Over many cycles, the undrained shear strength decreases to a minimal value, associated with the fully remolded state of the soil. During a calm period between two successive disturbance events, the excess pore pressure will dissipate, resulting in densification (i.e., a reduction of void ratio or moisture content) and recovery of the effective stress.

It has recently been recognized that this aspect of soil behavior can be explored through penetrometer or other model tests in the geotechnical centrifuge. White and Hodder (2010) formulated a framework to capture the effects of complete soil remolding and reconsolidation on penetrometer resistance by incorporating simple critical-state soil mechanics (CSSM) concepts. The framework fitted observations from a centrifuge T-bar penetrometer test involving three episodes of remolding interspersed by two events of reconsolidation.

This paper extends the previous work by adapting this framework to include reconsolidation within a cyclic episode, as opposed to postcyclic reconsolidation only as in White and Hodder (2010). This framework is then compared with data from a novel vertically oriented penetrometer (VOP). This device is pushed horizontally at a fixed embedment to infer the near-surface profile of soil strength. This device has been valuable in centrifuge model studies to determine lateral cross sections of soil strength following tests. With further development, it could prove useful to examine the lateral strength heterogeneity over the zone of a planned foundation footprint and to supplement point measurements of strength profile from conventional penetrometers, for example along pipeline routes. The design and method of analysis of the VOP is described in more detail in Sahdi et al. (2016).

Test Methodology

A series of VOP and T-bar tests were performed in kaolin (properties as given in Table 1), which was normally consolidated (NC) at an acceleration of $100g$ in the beam centrifuge in the University of Western Australia (UWA). The VOP (Fig. 1) is a cylindrical rod that is strain-gauged above the mudline to assess the lateral soil resistance on the buried part and therefore the soil strength based on the analysis of a laterally loaded pile as described in Sahdi et al. (2016).

A total of 10 VOP tests were conducted, which involved insertion of the device (at 0.5 mm/s) to a depth, z_T (distance from the mudline to the embedded tip of the VOP), followed by cycles of horizontal movement with a specified velocity, v, and horizontal amplitude, u (Table 2). These 10 VOP tests include 2 additional slow tests to those reported by Sahdi et al. (2016), designated in Table 2 as VOP_NC0330 and VOP_NC045. These tests were conducted at $v = 0.3$ mm/s and an embedment of 30 and 45 mm (model scale), respectively. Conventional cyclic T-bar tests were conducted, for reference soil-strength characterization, at a penetration rate of 1 mm/s using a T-bar with a diameter of 5 mm and a length of 20 mm (Table 2).

Shear Strength and Sensitivity of Sample

Fig. 2(a) shows the strength, s_u, derived from the T-bar penetration resistance, $q_{T-\text{bar}}$

[1]Senior Lecturer, Dept. of Civil Engineering, Faculty of Engineering, Univ. Malaysia Sarawak, 94300 Kota Samarahan Sarawak, Malaysia (corresponding author). E-mail: sfauzan@unimas.my

[2]Shell EMI Professor of Offshore Engineering, Centre for Offshore Foundation Systems, Univ. of Western Australia, Crawley, WA 6009, Australia.

[3]Professor, Centre for Offshore Foundation Systems, Univ. of Western Australia, Crawley, WA 6009, Australia.

Note. This manuscript was submitted on July 22, 2015; approved on August 23, 2016; published online on November 16, 2016. Discussion period open until April 16, 2017; separate discussions must be submitted for individual papers. This technical note is part of the ***Journal of Geotechnical and Geoenvironmental Engineering***, © ASCE, ISSN 1090-0241.

Table 1. Properties of UWA Kaolin

Property	Value	Reference
Specific gravity (G_s)	2.6	Boukpeti et al. (2012)
Plastic limit (PL)	28%	
Liquid limit (LL)	58%	
Coefficient of consolidation (c_v) (m^2/year)	2.6	Stewart (1991)
Normal consolidation line (NCL) or critical state line (CSL) slope (λ)	0.281	M. D. Richardson, personal communication (2007)
Specific volume at $\sigma'_v = 1$ kPa on NCL (N_{NCL})	3.72	
Unload–reload slope (κ)	0.06	

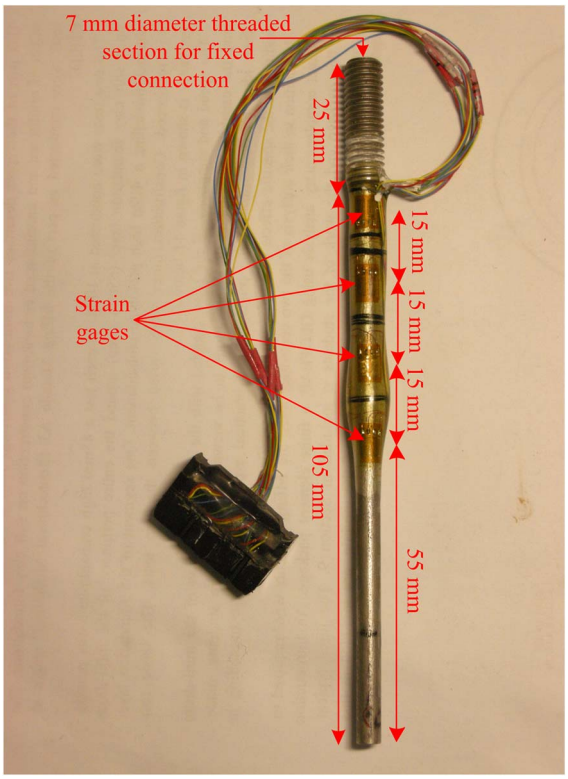

Fig. 1. Vertically oriented penetrometer (VOP) (adapted from Sahdi et al. 2016, © 2008 Canadian Science Publishing or its licensors; reproduced with permission)

$$s_u = \frac{q_{T-\text{bar}}}{N_{T-\text{bar}}} \quad (1)$$

Here, the s_u profile is derived by taking into account the transition from a shallow to deep failure mechanism of the T-bar (White et al. 2010).

The profiles of initial strength $s_{u-\text{in}}$ can be represented by the following equation:

$$s_{u-\text{in}} = k_{su} z \,(\text{kPa}) \quad (2)$$

where the best fit strength gradient, k_{su}, is 0.09 kPa/mm [Fig. 2(a)] at model scale (0.9 kPa/m at prototype scale).

The full cyclic resistance profiles allow the degradation in strength resulting from continuous cycles of penetration and extraction to be quantified using the degradation factor, D_f, defined as the shear strength at a particular cycle, s_{u-n}, normalized by the initial T-bar penetration strength, $s_{u-\text{in}}$. These strength values are extracted from the middepth of the vertical range during the cyclic tests. The cyclic variation in D_f is shown in Fig. 2(b). The cycle number, n, is calculated as recommended by Randolph et al. (2007): the first penetration is designated as $n = 0.25$ and n for subsequent extractions and penetrations is incremented by 0.5 ($n = 0.75$, 1.25, etc.). The sensitivity, S_t, is estimated as ~2.3 from the stabilized D_f limits, where $S_t = 1/D_f$.

Reconsolidation during Cyclic VOP Test

The lateral resistance during fast VOP horizontal translations, in which negligible pore pressure dissipation occurs was discussed by Sahdi et al. (2016). The present paper reports the full range of tests and is focused on the response in the middle position of each cyclic range and the influence of consolidation within the cycles.

Two examples of the full VOP soil resistance-displacement profiles for $z_T = 30$ mm are shown in Fig. 3. The soil resistance is expressed as the mean net pressure, q_h, which is the total resultant horizontal load, F_h, normalized by the projected area of the embedded VOP section. The horizontal displacement, u, is normalized with the VOP diameter, D_{VOP}, and the cycle numbering system is the same as for the T-bar. Tests VOP_NC3 ($v = 3$ mm/s) and VOP_NC0330 ($v = 0.3$ mm/s) involved a total of 9.75 and 26.75 cycles, respectively. The first VOP horizontal forward sweep ($n = 0.25$) in both tests shows a distinct peak, after which the resistance stabilizes at a displacement of $2D_{\text{VOP}}$.

The faster cyclic test VOP_NC3 [Fig. 3(a)] shows a decrease in the lateral resistance that matches the cyclic T-bar test [Fig. 2(a)],

Table 2. VOP and T-Bar Test Details (Adapted from Sahdi et al. 2016, © 2008 Canadian Science Publishing or Its Licensors. Reproduced with Permission)

Test reference	VOP embedment (z_T) (mm)	VOP horizontal displacement (u) (mm)	T-bar total vertical displacement (mm)	VOP horizontal cyclic distance (mm)	T-bar vertical cyclic depth (mm)	Test velocity (v) (mm/s)	Number of cycles (n)
T-bar_NC1	—	—	100	—	18–48	1	10.75
VOP_NC1	30	40	—	0–40	—	1	9.75
VOP_NC2	45	40	—	0–40	—	1	9.75
VOP_NC3	30	40	—	0–40	—	3	9.75
VOP_NC4	45	40	—	0–40	—	3	9.75
VOP_NC5	30	100	—	0–100	—	10	9.75
VOP_NC6	45	100	—	0–100	—	10	9.75
VOP_NC0330	30	20	—	0–20	—	0.3	26.75
VOP_NC0345	45	20	—	0–20	—	0.3	35.75
VOP_NC7	30	100	—	0–100	—	30	9.75
VOP_NC8	45	100	—	0–100	—	30	9.75
T-bar_NC2	—	—	60	—	29–49	1	10.75

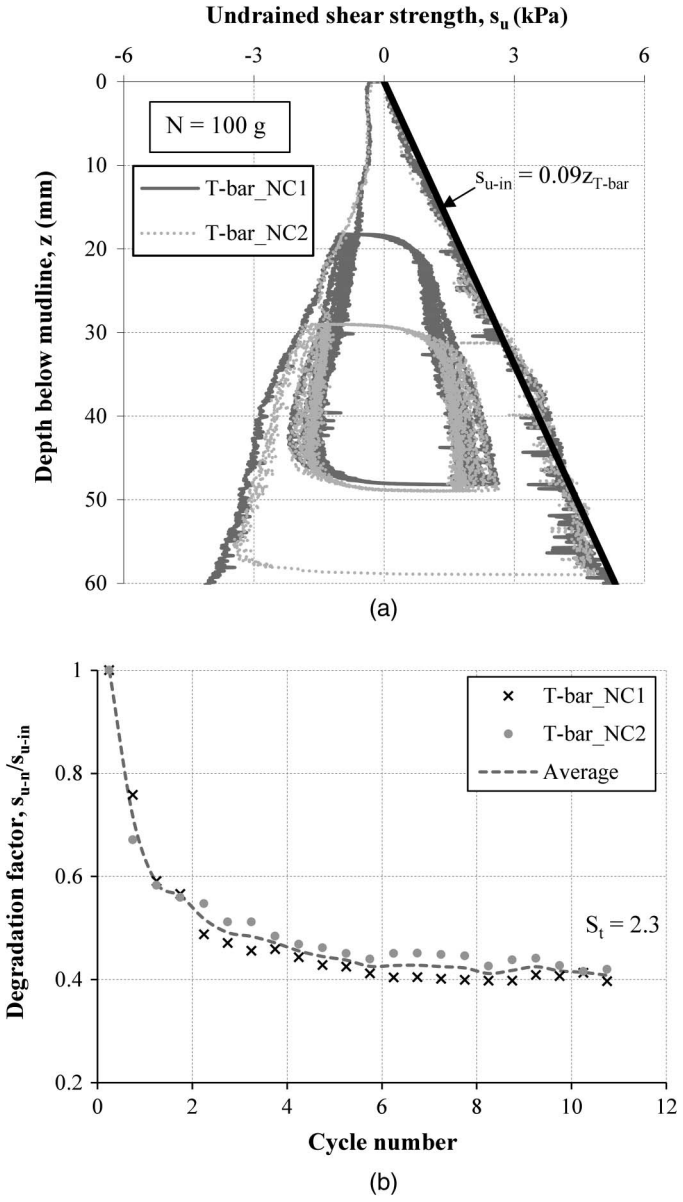

Fig. 2. T-bar cyclic tests results in NC sample: (a) cyclic tests profiles (adapted from Sahdi et al. 2016, © 2008 Canadian Science Publishing or its licensors; reproduced with permission); (b) T-bar strength degradation factor extracted from midpoint of cyclic test distance

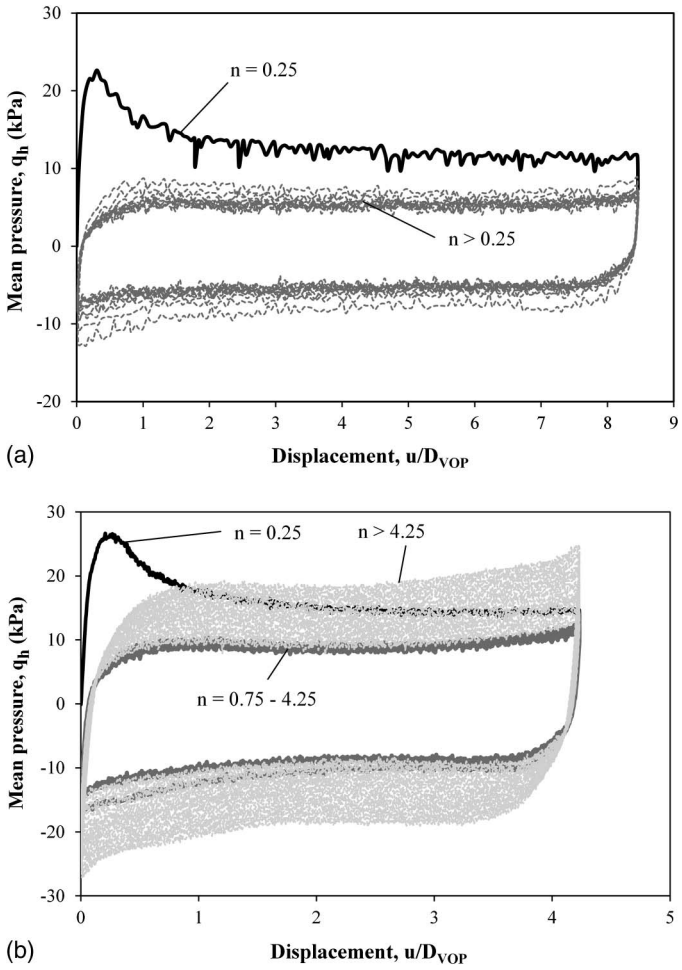

Fig. 3. Load-displacement response for test with $z_T = 30$ mm: (a) test VOP_NC3 ($v = 3$ mm/s); (b) test VOP_NC0330 ($v = 0.3$ mm/s)

indicating a similar remolding process. However, test VOP_0330 shows a distinctly different cyclic load-displacement profile [Fig. 3(b)]. After the first forward sweep, the soil resistance continuously decreases for cycle numbers 0.75–4.25, after which it increases steadily, surpassing even the initial steady resistance after many cycles.

The evolution of the resistance with cycle number and the dimensionless time factor, $T = c_v t/z_T^2$ for all tests are shown in Figs. 4(a and b) respectively. In Fig. 4(b), t is the time since cycle $n = 0.25$ and c_v is the coefficient of consolidation of the intact soil (Table 1). The midcycle VOP mean net resistance in each cycle, q_{h-n}, is normalized by the value in the first sweep ($n = 0.25$), $q_{h-0.25}$, to create the degradation factor, D_f, on the vertical axis, which is equivalent to D_f for the T-bar. For comparison, the average T-bar degradation curve [Fig. 2(b)], defined previously as $s_{u-n}/s_{u-\text{in}}$ is also included in Fig. 4(a).

The VOP responses match that of the T-bar when the VOP is translated horizontally at $v \geq 3$ mm/s. However, different profiles of resistance are evident for the VOP tests at v of $0.3 - 1$ mm/s. These slower tests do not reach the same low remolded value, and the slowest tests actually show a significant rise in resistance which is more marked in the shallow cases, reflecting an increase in consolidation time, T, as can be seen in Fig. 4(b).

These observations indicate the influence of reconsolidation of the soil between disturbance as the VOP passes, since the cyclic test distance and velocity affect the corresponding time interval. Also, the embedment affects the drainage path length, which influences the pore-pressure dissipation rate.

Having presented the experimental results, the remainder of this paper describes how the results can be replicated analytically using a simple framework for remolding and reconsolidation.

Interpretation and Back-Analysis

Strength Evolution due to Drainage between Shearing

The effect of drainage between undrained shearing episodes can be accounted for using a form of the framework outlined by White and Hodder (2010). In essence, this framework links the degradation of soil strength during remolding to the accumulation of positive excess pore pressure, and the recovery of soil strength is linked to the dissipation of that excess pore pressure. A critical-state framework

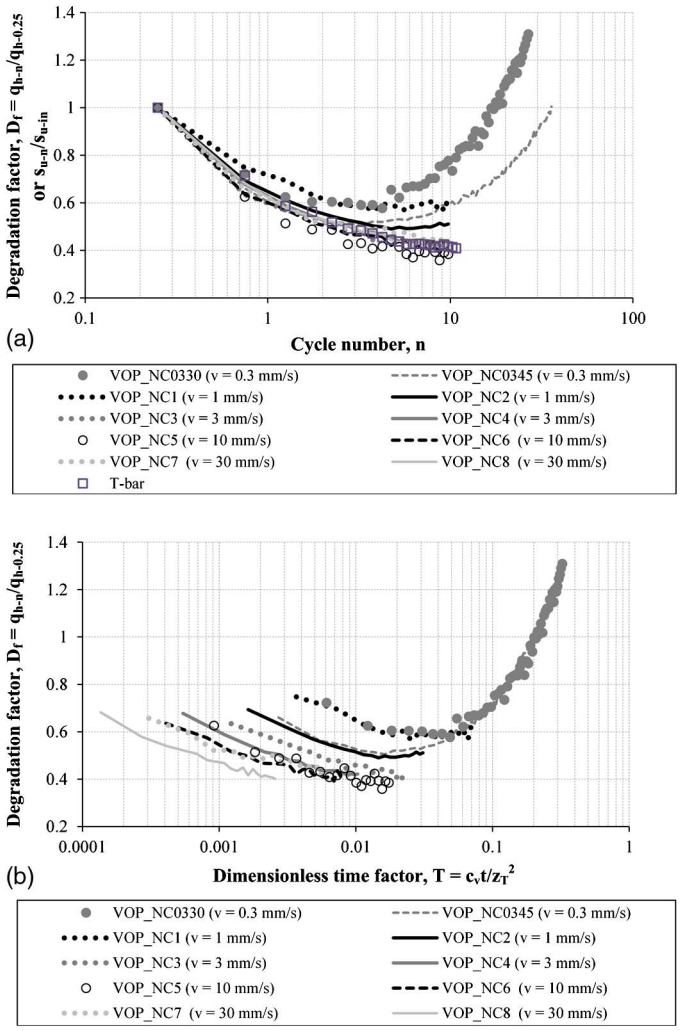

Fig. 4. Evolution of VOP steady lateral resistance with (a) cycle number; (b) dimensionless time

is used to link changes in moisture content (caused by dissipation) to changes in undrained strength.

Fig. 5 shows the idealized effective stress path of a representative soil element in specific volume (v)–vertical effective stress (σ'_v) space during a cyclic VOP episode based on the same simplifications used by White and Hodder (2010). The soil strength is assumed to be governed solely by the current vertical effective stress.

The undisturbed state lies on the normal compression line (NCL) (Point A in Fig. 5). The in situ specific volume can be calculated from Eq. (3) as follows:

$$\nu = N_{\text{NCL}} - \lambda \ln \sigma'_{vo} \tag{3}$$

where N_{NCL} = specific volume on the NCL at $\sigma'_v = 1$ kPa; σ'_{vo} = initial vertical effective stress; and λ = slope of the NCL.

The model is based on two failure lines in specific volume–effective stress space. The critical state line (parallel to the NCL with slope λ) is assumed to be reached (Point B in Fig. 5) when the soil element first fails (in the case of a T-bar or VOP test, this corresponds to the $n = 0.25$ shearing event). During subsequent undrained cycles (no reconsolidation is allowed between two successive shearing), the stress point progressively migrates to a second failure line (Point B in Fig. 5), defined as the remolded state line (RSL). The RSL represents the lowest stress state achievable at

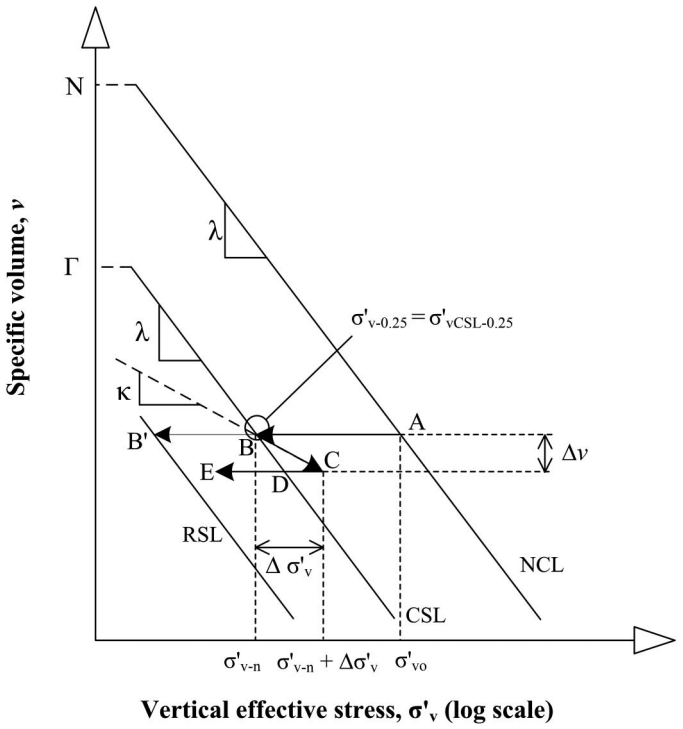

Fig. 5. Idealized stress path in $v - \sigma'_v$ space

any given v, and the stress spacing ratio between the RSL and the CSL is equal to the soil sensitivity, S_t.

During a set of undrained VOP cycles, the positive excess pore pressure results in a current vertical effective stress, σ'_{v-n} (subscript n denotes cycle number), which is a proportion of the stress at the critical state line corresponding to the current specific volume, v

$$\sigma'_{v-n} = R\sigma'_{\text{vCSL}-n} \tag{4}$$

where $\sigma'_{\text{vCSL}-n}$ = vertical effective stress on the CSL at the current n, and so is linked to the current specific volume by

$$\sigma'_{\text{vCSL}-n} = e^{\Gamma - v/\lambda} \tag{5}$$

where Γ = CSL specific volume at $\sigma'_v = 1$ kPa.

The parameter R controls the position of the failure stress, σ'_{v-n} between the CSL and the RSL and can be written as

$$R = \frac{1}{S_t} + \left(1 - \frac{1}{S_t}\right) e^{-3(n-0.25)/N_{95}} \tag{6}$$

where S_t = soil sensitivity; and N_{95} = number of VOP cycles to cause 95% degradation of the initial resistance when negligible reconsolidation occurs during a cyclic episode. In this way, the progress of the failure stress point from the CSL to the RSL is linked to the degradation in resistance seen in undrained cyclic T-bar or VOP tests. From Eqs. (4)–(6), it can be seen that at cycle $n = 0.25$, $\sigma'_{v-0.25} = \sigma_{\text{vCSL}-0.25}$. Up to this point the framework simply yields an exponential decay in penetrometer resistance with a ratio S_t between the initial and final values. This is consistent with previous interpretations of cyclic penetrometer tests, such as those carried out by Einav and Randolph (2005) and Zhou and Randolph (2009). However, drainage between two shearing events must also be considered. Between VOP shearing events the current excess pore pressure (given by $\sigma'_{vo} - \sigma'_{v-n}$) may partially dissipate causing an increase in vertical stress of

$$\Delta\sigma'_v = \mathrm{U}(\sigma'_{vo} - \sigma'_{v-n}) \quad (7)$$

where U = degree of excess pore pressure dissipation, which is derived from the elapsed time. The pore-pressure dissipation leads to a decrease in specific volume, Δv (Points B to C in Fig. 5):

$$\Delta v = -\kappa \ln\left(\frac{\sigma'_{v-n} + \Delta\sigma'_v}{\sigma'_{v-n}}\right) \quad (8)$$

where the magnitude of Δv depends on the reconsolidation slope κ.

After dissipation, the next VOP shearing event moves the effective stress to a position between the CSL and the RSL that depends on the cumulative number of cycles [Eq. (6)] and the current specific volume (Position E in Fig. 5). At any given σ'_{v-n} during shearing, the operative strength, s_{u-op} can be calculated from the strength parameter, μ, as

$$s_{u-\mathrm{op}} = \mu\sigma'_{v-n} \quad (9)$$

In the back-analysis described in this paper, the lateral soil resistance at any depth on the VOP embedded portion is then calculated as $10.5s_{u-op}$.

Dissipation of Excess Pore-Water Pressure

The rate of increase in soil resistance for the slower tests is higher with decreasing test embedment (Fig. 4). This suggests that the dissipation of positive excess pore pressure primarily occurs vertically, and is controlled by the total VOP embedment depth, z_T. Following the first horizontal VOP sweep and in accordance to Eqs. (4)–(6), the excess pore pressure will be equal to $\sigma'_{vo} - \sigma'_{v-0.25}$. This creates a distribution of excess pore pressure that is triangular in shape, increasing linearly from the mudline. If dissipation of the excess pore pressure is assumed to occur only towards the free water boundary at the mudline, the remaining excess pore pressure (u_{e-tc}) at a given depth below the mudline (z) up to the total VOP embedment depth (z_T) can be estimated using the Fourier-series solution of Terzaghi and Frohlich (1936)

$$u_{e-\mathrm{tc}} = \sum_{x=1}^{\infty}\left[\left(\frac{8u_{\mathrm{ezT}}}{x^2\pi^2}\right)\sin\left(\frac{x\pi}{2}\right)\sin\left(\frac{x\pi z}{2z_T}\right)e^{-x^2\pi^2 T/4}\right] \quad (10)$$

where x = number of Fourier-series terms; and u_{ezT} = excess pore pressure at $z = z_T$. The elapsed reconsolidation time, t_c, is expressed as a dimensionless time factor, T

$$T = \frac{c_v t_c}{z_T^2} \quad (11)$$

The resulting degree of consolidation, U, at a given depth is then

$$U = 1 - \frac{u_{e-\mathrm{tc}}}{u_{\mathrm{ez-t0}}} \quad (12)$$

where u_{ez-t0} = excess pore pressure generated at a particular depth below the mudline. For convenience, the degree of consolidation U inferred for the first cyclic episode is assumed constant for all subsequent cyclic episodes.

This method to estimate the degree of consolidation predicts the change in specific volume, v [Eqs. (7) and (8)] at a particular depth z below the mudline during reconsolidation. The operative strength, s_{u-op}, at a given depth during a subsequent VOP pass can then be determined based on the current v [Eqs. (4)–(6) and (9)]. This is then factored by the VOP bearing factor, $N_h = 10.5$ and integrated over the depth of the VOP to assess the mean lateral resistance, q_{h-n}.

Table 3. Framework Parameters

Parameter	Value
Operative normally consolidated strength ratio $(s_u/\sigma'_v)_{nc}$	0.15
Friction factor (μ) (White and Hodder 2010)	0.7
CSL specific volume at $\sigma'_v = 1$ kPa (Γ)	3.29
Soil sensitivity (S_t)	2.3
Rate of strength degradation (N_{95})	2.5

Parameters for Back-Analysis

The parameters used to apply this model to the VOP tests include N_{NCL}, κ, λ, and c_v, which have been introduced previously in Table 1. The remaining model parameters required are presented in Table 3. Here, Γ may be estimated as (White and Hodder 2010)

$$\Gamma = N_{\mathrm{NCL}} + \lambda\ln\left[\left(\frac{s_u}{\sigma'_v}\right)_{\mathrm{nc}}\mu^{-1}\right] \quad (13)$$

where $(s_u/\sigma'_v)_{nc}$ = normally consolidated strength ratio, which is taken as 0.15 based the T-bar strength profile and soil unit weight; and μ is taken as 0.7 (White and Hodder 2010). This would result in $\Gamma = 3.29$. Parameters S_t and N_{95} control the spacing of the CSL and RSL and the rate at which pore pressure accumulates during VOP cycles [Eq. (6)]. The test data at $v > 1$ mm/s (during which negligible pore pressure dissipation occurred) were used to derive these parameters by fitting the calculated profile of $q_{h-n}/q_{h-0.25}$ [Eq. (6)] to the data. The best-fit S_t and N_{95} values are 2.3 and 2.5, respectively, which are consistent with previous studies using T-bar tests in UWA kaolin (e.g., Sahdi et al. 2010, 2014).

Comparison of Model with Test Data

Comparisons between the measured and predicted mid-cycle lateral resistance for VOP tests at $v = 1$ and 0.3 mm/s are shown in Fig. 6 (30 mm embedment) and Fig. 7 (45 mm embedment).

The model agrees well with the measured data for tests at $v = 1$ mm/s (VOP_NC1 and VOP_NC2). The dimensionless time factors between the VOP passing the midcycle point are $T = 0.0037$ and 0.0016 for tests VOP_NC1 and VOP_NC2, respectively. These times correspond to dissipations of only $U = 6.8$ and 4.6% at the deepest point of $z = z_T$. For comparison purposes, the response with no allowance for reconsolidation is also shown, and predicts lower resistance.

The performance of the model when compared to the test data at v = 0.3 mm/s [Figs. 6(b) and 7(b)] is strongly influenced by the reconsolidation element of the model. The general trend of initial softening, followed by gentle hardening, is captured well by the model. However, using the base case input parameters (Tables 1 and 3), the model underpredicts the measured q_{h-n} for tests VOP_NC0330 and VOP_NC0345 by about 30% at each final cycle. Again, for comparison purposes, the model response when no allowance for reconsolidation is also shown.

There are two likely explanations for this discrepancy. As mentioned previously, the degree of consolidation U for each reconsolidation event is estimated based on the triangular excess pore-pressure distribution generated during cycle number $n = 0.25$. In fact, as repeated events of disturbance and reconsolidation increase, this distribution is no longer triangular. This decreases the accuracy of the model if consolidation occurs at a higher rate (as seen for tests VOP_NC0330 and VOP_NC0345).

Alternatively, the assumed parameters that control dissipation and strengthening may be inaccurate, given that the elemental soil properties are being applied to a model that idealizes the flow

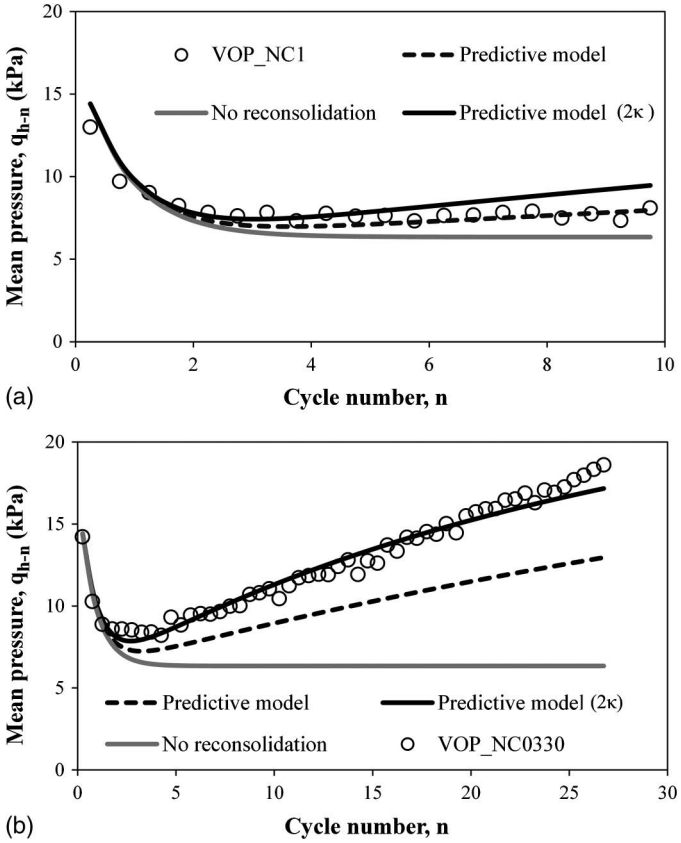

Fig. 6. Comparison between model and VOP centrifuge data for tests at 30-mm embedment and velocities of (a) 1 mm/s (test VOP_NC1); (b) 0.3 mm/s (test VOP_NC0330)

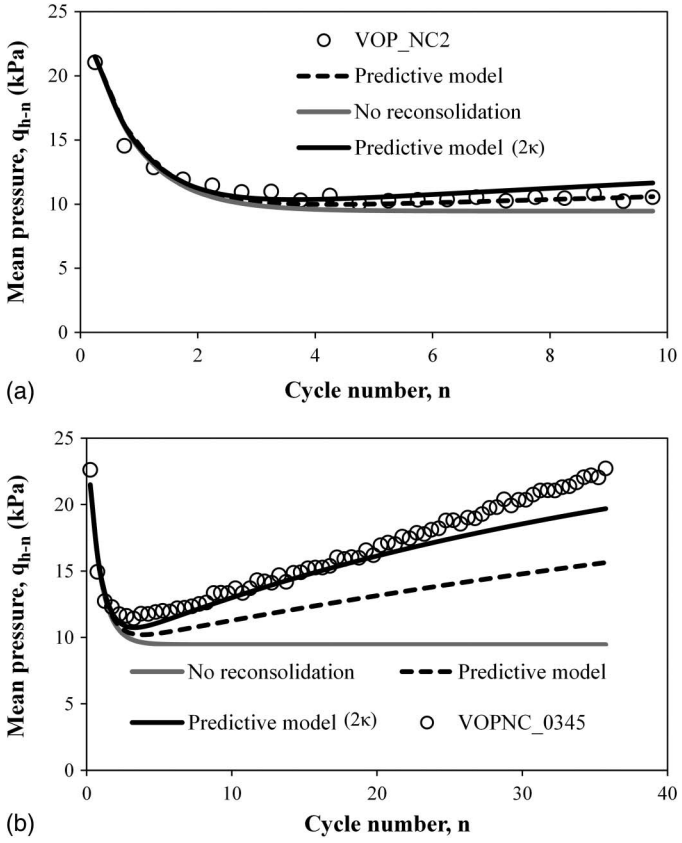

Fig. 7. Comparison between model and VOP centrifuge data for tests at 45-mm embedment and velocities of (a) 1 mm/s (test VOP_NC2); (b) 0.3 mm/s (test VOP_NC0345)

around the VOP via the state of a single representative soil element. Even at a soil-element level, alternative assumptions may be appropriate. For example, a higher reconsolidation slope κ may be more applicable. This is in accordance to the experimental findings using triaxial and simple shear tests (Ohara and Matsuda 1988; Yasuhara and Andersen 1991; Hyde et al. 2007) where reconsolidation stress paths have slopes varying from 1.5κ up to magnitudes comparable to the slope of the NCL or CSL—λ. The sensitivity of the model behavior to this parameter is illustrated in Figs. 6 and 7, where additional responses based on vertical dissipation using a higher (by a factor of 2) value of κ are illustrated. In this case the agreement is excellent for the tests at $v = 0.3$ mm/s (VOP_NC0330 and VOP_NC0345), with an underprediction of 8–11% at the last respective cycles only. However, the model predicts a slightly faster rate of increase in q_{h-n} for the tests at $v = 1$ mm/s (VOP_NC1 and VOP_NC2).

Overall, the framework can capture the underlying trend of VOP resistance evolution during a cyclic episode when reconsolidation in between shearing events is permitted.

Conclusions

A series of centrifuge tests utilizing a novel vertically oriented penetrometer (VOP) to assess the changing strength of clay during shearing and reconsolidation have been reported. In these tests, the VOP was embedded at 30 and 45 mm depth (6.4–9.5 VOP diameters), and the horizontal cyclic velocities were 0.3, 1, 3, 10, and 30 mm/s for each test embedment. For test velocities of 3, 10, and 30 mm/s, similar load degradation profiles to that inferred from a T-bar cyclic test are observed. However, for tests velocities of 0.3 and 1 mm/s, it was found that the VOP resistance rises after the first few cycles, reflecting the dissipation of excess pore pressures generated during each cycle, causing reconsolidation. The VOP resistance even surpasses the initial value after many cycles for the longest duration tests, illustrating that the strengthening effect of reconsolidation can eclipse the weakening effect of remolding.

A previously published framework that combines the effects of disturbance and reconsolidation is used to back-analyze the centrifuge data. By incorporating a one-dimensional consolidation solution into this framework to estimate the degree of consolidation between two VOP passes, good predictions of the changing measured VOP resistance can be made.

In summary, these results show how the increase in soil strength during a cyclic shearing episode can be quantified, allowing for the competing effects of remolding and reconsolidation. The data and the framework used in the back-analysis are relevant to other cyclic processes found in offshore engineering, including the cyclic response of pipelines and piles, as well as the reinstallation of spudcan foundations. The simple framework outlined in this paper and the VOP as a novel soil characterization tool offer a basis to estimate the significant changes in soil strength that can occur during cyclic loading events that span a timeframe comparable to the consolidation process.

Acknowledgments

This research was supported by the Minerals and Energy Research Institute of Western Australia, and by BP, BHP Billiton, Chevron, Petrobras, Shell, and Woodside. The financial support of all the

participants is gratefully acknowledged. The authors are grateful to Noel Boylan, Don Herley, Phil Hortin, and Shane De Catania for their technical assistance. The first author is also grateful for the financial support received from the Ministry of Higher Education Malaysia (MOHE) and Universiti Malaysia Sarawak (UNIMAS).

Notation

The following symbols are used in this paper:

c_v = coefficient of consolidation;
D_f = degradation factor;
D_{VOP} = VOP diameter;
F_h = VOP horizontal resultant load;
G_s = specific gravity;
k_{su} = undrained strength gradient;
N_{95} = number of VOP cycles required to achieve 95% degradation of the initial VOP resistance;
N_{NCL} = specific volume at $\sigma'_v = 1$ kPa on the normal compression line;
$N_{T-\mathrm{bar}}$ = T-bar bearing factor;
n = T-bar or VOP cycle number;
q_h = VOP mean net pressure;
$q_{h-0.25}$ = VOP mean net pressure at cycle number $n = 0.25$;
q_{h-n} = VOP mean net pressure at any cycle number n;
$q_{T-\mathrm{bar}}$ = T-bar resistance;
R = ratio of the current vertical effective stress, σ'_{v-n} to current vertical effective stress on the critical state line, $\sigma'_{\mathrm{vCSL}-n}$ at any cycle number, n;
S_t = soil sensitivity;
$s_{u-\mathrm{in}}$ = undrained strength from the initial T-bar penetration;
s_{u-n} = undrained strength at a particular cycle number n;
s_{u-op} = operative undrained strength;
$(s_u/\sigma'_v)_{nc}$ = normally consolidated undrained strength ratio;
T = dimensionless time factor;
t = elapsed time since the first VOP pass ($n = 0.25$);
t_c = elapsed time between two successive VOP passes;
u = VOP horizontal displacement;
U = degree of excess pore pressure dissipation;
u_{e-tc} = excess pore pressure at any t_c;
u_{ezT} = excess pore pressure at the maximum VOP embedment, z_T;
u_{ez-t0} = excess pore pressure generated at any depth after shear;
v = T-bar or VOP test velocity;
v = specific volume of soil;
x = number of Fourier-series terms;
z = depth below the mudline;
z_T = VOP total embedment (measured from the VOP tip to the mudline);
Γ = specific volume on the critical state line at $\sigma'_v = 1$ kPa;
$\Delta\sigma'_v$ = change in vertical effective stress;
Δv = change in specific volume;
μ = strength parameter;
κ = unload-reload slope;
λ = slope of the normal consolidation line or the critical state line;
σ'_v = vertical effective stress;
$\sigma'_{\mathrm{vCSL}-n}$ = vertical effective stress on the critical state line at any cycle number, n;
σ'_{v-n} = vertical effective stress at any cycle number, n; and
σ'_{vo} = initial vertical effective stress.

References

Boukpeti, N., White, D. J., Randolph, M. F., and Low, H. E. (2012). "Strength of fine-grained soils at the solid-fluid transition." *Géotechnique*, 62(3), 213–226.

Einav, I., and Randolph, M. F. (2005). "Combining upper bound and strain path methods for evaluating penetration resistance." *Int. J. Numer. Methods Eng.*, 63(14), 1991–2016.

Hyde, A. F. L., Higuchi, T., and Yasuhara, K. (2007). "Postcyclic recompression, stiffness, and consolidated cyclic strength of silt." *J. Geotech. Geoenviron. Eng.*, 10.1061/(ASCE)1090-0241(2007)133:4(416), 416–423.

Ohara, S., and Matsuda, H. (1988). "Study on the settlement of saturated clay layer induced by cyclic shear." *Soils Found.*, 28(3), 103–113.

Randolph, M. F., Low, H. E., and Zhou, H. (2007). "In situ testing for design of pipeline and anchoring systems." *Proc., 6th Int. Conf. on Offshore Site Investigation and Geotechnics*, Society for Underwater Technology, London, 27–38.

Sahdi, F., Boylan, N., White, D. J., and Gaudin, C. (2010). "The influence of coloured dyes on the undrained shear strength of kaolin." *7th Int. Conf. on Physical Modelling in Geotechnics*, Taylor & Francis Group, London.

Sahdi, F., Gaudin, C., and White, D. J. (2014). "Strength properties of ultra-soft kaolin." *Can. Geotech. J.*, 51(4), 420–431.

Sahdi, F., White, D. J., Gaudin, C., Randolph, M. F., and Boylan, N. (2016). "Laboratory development of a vertically oriented penetrometer for shallow seabed characterization." *Can. Geotech. J.*, 53(1), 93–102.

Stewart, D. P. (1991). "Lateral loading of piled bridge abutments due to embankment construction." Ph.D. thesis, Univ. of Western Australia, Perth, Australia.

Terzaghi, K., and Frohlich, O. K. (1936). *Theorie der Setzung von Tonschichten: Eine Einfuhrung in die Analytische Tonmechanik*, Franz Deuticke, Leipzig, Germany (in German).

White, D. J., Gaudin, C., Boylan, N., and Zhou, H. (2010). "Interpretation of T-bar penetrometer tests at shallow embedment and in very soft soils." *Can. Geotech. J.*, 47(2), 218–229.

White, D. J., and Hodder, M. (2010). "A simple model for the effect on soil strength of episodes of remoulding and reconsolidation." *Can. Geotech. J.*, 47(7), 821–826.

Yasuhara, K., and Andersen, K. H. (1991). "Recompression of normally consolidated clay after cyclic loading." *Soils Found.*, 31(1), 83–94.

Zhou, H., and Randolph, M. F. (2009). "Numerical investigations into cycling of full-flow penetrometers in soft clay." *Géotechnique*, 59(10), 801–812b.